X-ray crystallographic snapshots of reaction intermediates in the G117H mutant of human butyrylcholinesterase, a nerve agent target engineered into a catalytic bioscavenger

Florian Nachon, Eugenie Carletti, Marielle Wandhammer, Yvain Nicolet, Lawrence M Schopfer, Patrick Masson, Oksana Lockridge

▶ **To cite this version:**

Florian Nachon, Eugenie Carletti, Marielle Wandhammer, Yvain Nicolet, Lawrence M Schopfer, et al.. X-ray crystallographic snapshots of reaction intermediates in the G117H mutant of human butyrylcholinesterase, a nerve agent target engineered into a catalytic bioscavenger. Biochemical Journal, 2011, 434 (1), pp.73-82. 10.1042/BJ20101648 . hal-00560692

HAL Id: hal-00560692
https://hal.science/hal-00560692v1

Submitted on 29 Jan 2011

HAL is a multi-disciplinary open access archive for the deposit and dissemination of scientific research documents, whether they are published or not. The documents may come from teaching and research institutions in France or abroad, or from public or private research centers.

L'archive ouverte pluridisciplinaire **HAL**, est destinée au dépôt et à la diffusion de documents scientifiques de niveau recherche, publiés ou non, émanant des établissements d'enseignement et de recherche français ou étrangers, des laboratoires publics ou privés.

Biochemical Journal Immediate Publication. Published on 19 Nov 2010 as manuscript BJ20101648

X-ray crystallographic snapshots of reaction intermediates in the G117H mutant of human butyrylcholinesterase, a nerve agent target engineered into a catalytic bioscavenger.

Florian NACHON*, Eugenie Carletti*, Marielle Wandhammer*, Yvain Nicolet†, Lawrence M. Schopfer‡, Patrick Masson*‡ and Oksana Lockridge‡

* Cellule Enzymologie, Département de Toxicologie, Institut de Recherche Biomédicale des Armées - CRSSA, 24 avenue des Maquis du Grésivaudan, 38700 La Tronche, France
† Laboratoire de Cristallogenèse et Cristallographie des Protéines. Institut de Biologie Structurale (CEA-CNRS-UJF). 41 rue Jules Horowitz, 38027 Grenoble, France
‡ Eppley Institute and Department of Biochemistry and Molecular Biology, University of Nebraska Medical Center, Omaha, Nebraska 68198-5950,

Running title. Structure of the human butyrylcholinesterase G117H mutant.

Corresponding author:
Dr. Florian Nachon,
Unité PhyTAN, Cellule Enzymologie, Département de Toxicologie,
Institut de Recherche Biomédicale des Armées - CRSSA,
24 av des Maquis du Grésivaudan, 38700 La Tronche, France.
Tel: +33476636959 / Fax: +33476636962
E-mail: florian@nachon.net

THIS IS NOT THE VERSION OF RECORD - see doi:10.1042/BJ20101648

Accepted Manuscript

Licenced copy. Copying is not permitted, except with prior permission and as allowed by law.
© 2010 The Authors Journal compilation © 2010 Portland Press Limited

Biochemical Journal Immediate Publication. Published on 19 Nov 2010 as manuscript BJ20101648

Abstract

Organophosphylates (OPs) exert their acute toxicity through inhibition of acetylcholinesterase, by phosphylation of the catalytic serine. Engineering of human butyrylcholinesterase by substitution of histidine for glycine at position 117 led to the creation of OP hydrolase activity. But the lack of structural information and poor understanding of the hydrolytic mechanism of G117H has hampered further improvements in the catalytic activity. We solved the crystallographic structure of the G117H mutant with a variety of ligands in the active site. A sulfate anion bound to the active site suggested the positioning for an OP prior to phosphylation. A fluoride anion was found in the active site when NaF was added to the crystallization buffer. In the fluoride complex, the imidazole ring from His117 was substantially shifted adopting a relaxed conformation most likely close to that of the unliganded mutant enzyme. Additional X-ray structures were obtained from the transient covalent adducts formed upon reaction of G117H with the OPs echothiophate and VX. The position of His117 shifted in response to the introduction of these adducts, overlaying the phosphylserine. These structural data suggest that the dephosphylation mechanism involves either a substantial conformational change of His117 or an adjacent nucleophilic substitution by water.

Keywords: acetylcholinesterase, butyrylcholinesterase, bioscavenger, reactivation, engineering, organophosphorus

THIS IS NOT THE VERSION OF RECORD - see doi:10.1042/BJ20101648

Accepted Manuscript

Licenced copy. Copying is not permitted, except with prior permission and as allowed by law.
© 2010 The Authors Journal compilation © 2010 Portland Press Limited

Biochemical Journal Immediate Publication. Published on 19 Nov 2010 as manuscript BJ20101648

Abbreviations used: AChE, Acetylcholinesterase; BChE, Butyrylcholinesterase; ChE, Cholinesterase; CHO, Chinese hamster ovary; MES, 2-(N-morpholino)ethanesulfonic acid; OP, Organophosphylate; DEP, diethoxyphosphoryl; VX, O-ethyl-S-[2[bis(1-methyl-ethyl) amino] ethyl] methylphosphonothioate; LD50, lethal dose for 50% of the population.

THIS IS NOT THE VERSION OF RECORD - see doi:10.1042/BJ20101648

Accepted Manuscript

Licenced copy. Copying is not permitted, except with prior permission and as allowed by law.
© 2010 The Authors Journal compilation © 2010 Portland Press Limited

Biochemical Journal Immediate Publication. Published on 19 Nov 2010 as manuscript BJ20101648

THIS IS NOT THE VERSION OF RECORD - see doi:10.1042/BJ20101648

Introduction

Recent progress in the understanding of enzyme catalysis, through the use of structural biology and molecular modeling has opened a new era in protein engineering. It is now possible to develop rational strategies for modifying enzymes to confer upon them the ability to catalyze reactions for which they were not originally designed [1]. Human butyrylcholinesterase (BChE; EC 3.1.1.8) is an enzyme for which modifying the catalytic activity has been an ongoing subject of interest. This enzyme is related to acetylcholinesterase (AChE; EC 3.1.1.7), the enzyme that terminates the action of the neurotransmitter acetylcholine at postsynaptic membranes and neuromuscular junctions. BChE differs from AChE by its substrate specificity and inhibitor sensitivity [2, 3]. Although BChE is present in numerous vertebrate tissues, its physiological role remains unclear [4].

Considerable interest has been shown to BChE because it hydrolyzes a wide range of toxic esters, including heroin and cocaine, and because it scavenges toxic organophosphylate pesticides and nerve agents [5-7]. A large effort has been expended to improve its ability to hydrolyze these compounds. In this regard, it is noteworthy to mention that redesign of the active site improved its (-)-cocaine hydrolase activity by 2000-fold, turning it into a very efficient cocaine detoxifying tool [8]. This redesign was based on hybrid quantum mechanical/ molecular mechanical (QM/MM) studies aimed at finding ways to stabilize the acylation transition state of the cocaine hydrolysis reaction.

Reaction of cholinesterases with organophosphorus compounds (OPs) is another area in which modification of the native cholinesterase activity has received considerable attention. Interest in this area is a consequence of the irreversible inhibition of AChE (at the neuronal synapses and neuromuscular junctions) by organophosphorus compounds which leads to accumulation of acetylcholine and results in paralysis, seizures, and other symptoms of the cholinergic syndrome. Under extreme conditions, inhibition of AChE can lead to death [9]. Native plasma BChE works well as a stoichiometric bioscavenger because it reacts very efficiently with organophosphorus compounds, thus trapping them as a one-to-one complex in the blood stream before they can reach synaptic AChE. Injection of wild-type BChE *iv* or *im* protects animals against 3 to 5 LD50 doses of the nerve agents soman, VX, and tabun [10]. BChE purified from human plasma (Baxter Healthcare Corporation) or produced in the milk of transgenic goats [11] has successfully completed clinical trials and is about to reach the market as a bioscavenger for pretreatment against OP intoxication. A BChE dose up to 250 mg / 70 kg is required to achieve efficient protection of humans following a challenge with 1 LD50 of OPs[12]. Thus, a large amount of enzyme is necessary to get an efficient protection. This is due to the stoichiometric and irreversible nature of the reaction between the OP and butyrylcholinesterase, and to the unfavorable OP/BChE mass ratio. Such large doses are expensive, and will prevent the widespread use of wild-type BChE as a pretreatment. Research efforts now are devoted to circumventing this limitation by developing catalytic bioscavengers able to hydrolyze OPs [13].

Very early in the study of OP inhibition of cholinesterases, it was suggested that OP inhibitors could be considered as hemisubstrates of cholinesterases because formation of the enzyme-inhibitor complex was efficient but the dephosphylation was not. Slow dephosphylation was presumed to be a consequence of there being no amino acid groups at the appropriate positions to catalyze hydrolysis by in-line nucleophilic attack of water [14]. The idea of introducing a residue into the active site, that was capable of catalyzing the dephosphylation step, followed. In principle, after such a modification, OPs would become full substrates for the modified cholinesterase, or in other words, the added residue would turn the cholinesterase into an organophospho-hydrolase, i.e. a catalytic bioscavenger [15].

This approach proved to be qualitatively successful. BChE was shown to gain OP hydrolase activity when a histidine was substituted for glycine at position 117 [16, 17]. The G117H mutant is remarkably efficient at hydrolyzing echothiophate, having a catalytic rate constant, $k_{cat} = 0.75$ min^{-1} in 0.1 M potassium phosphate, pH 7.0, 25°C. G117H can also hydrolyze the nerve agents sarin, VX, and additionally soman if a second mutation (E197Q) is introduced to prevent fast aging of the conjugate [18]. Dephosphylation remains the rate-limiting step with $k_{cat} = 5.2 \times 10^{-3}$ min^{-1} for sarin, 7.2×10^{-3} min^{-1} for VX, and 77.0×10^{-3} min^{-1} for the most toxic isomer of soman (P_SC_S) (0.067 M phosphate buffer, pH

Accepted Manuscript

Licenced copy. Copying is not permitted, except with prior permission and as allowed by law.
© 2010 The Authors Journal compilation © 2010 Portland Press Limited

Biochemical Journal Immediate Publication. Published on 19 Nov 2010 as manuscript BJ20101648

7.5, 25 °C). Furthermore, it has been shown that transgenic mice expressing the G117H mutant are resistant to OP [19]. Although G117H/E197Q is generally considered to reactivate too slowly to be of general use as a catalytic bioscavenger for nerve agents, it provides an improvement over the native enzyme. Spontaneous reactivation of soman-, sarin- or VX- inhibited G117H/E197Q replenishes half of the affected enzyme in about 10 minutes [18]. This could be lifesaving in a scenario where successive exposures to these OPs occur.

To date, more than sixty BChE mutants have been made in an effort to improve the OP hydrolase activity of the original G117H mutant. It was found that G117D, G117E, L286H, and several G117H-based double and triple mutants were capable of hydrolyzing echothiophate [20]. However, G117H remains the most efficient mutant by at least two orders of magnitude. One reason for this relative failure to find an improved mutant is that the dephosphylation mechanism is poorly understood. Knowledge of the structure of the active site of G117H now appears to be critical in order to understand the catalytic mechanism and to design more efficient G117H-based mutants. An indication of the pressing need for an experimentally determined structure of the active site of G117H is provided by two recent publications [21, 22] in which the three dimensional structure of the G117H BChE mutant was determined computationally. Though they are interesting, such models cannot replace an experimental structure.

Here we present the X-ray structure of the G117H mutant, the structures of the transient covalent adducts formed upon reaction of G117H with echothiophate and VX (Scheme 1), and the structure of a fluoride complex which was the consequence of an attempt to create a transition-state phosphate analog in the form of MgF_3^-. These crystal structures give a true picture of the active site of G117H under a variety of conditions, and provide the essential information needed to perform QM/MM studies aimed at designing mutants with improved hydrolytic capabilities.

THIS IS NOT THE VERSION OF RECORD - see doi:10.1042/BJ20101648

Accepted Manuscript

Licenced copy. Copying is not permitted, except with prior permission and as allowed by law.
© 2010 The Authors Journal compilation © 2010 Portland Press Limited

Biochemical Journal Immediate Publication. Published on 19 Nov 2010 as manuscript BJ20101648

THIS IS NOT THE VERSION OF RECORD - see doi:10.1042/BJ20101648

Experimental

Materials

VX, O-ethyl-S-[2[bis(1-methyl-ethyl) amino] ethyl] methylphosphonothioate, was obtained from the Centre DGA Maîtrise NRBC (Vert-le-Petit, France). VX is highly toxic. It belongs to schedule 1 Chemicals as defined in the Chemical Weapons Convention. All work with VX is regulated by that convention. Echothiophate, O-diethyl-S-(2-trimethylammonium ethyl) phosphorothioate, was obtained from Biobasal (Basel, Switzerland). The handling of VX and echothiophate is dangerous and requires suitable personal protection, training, and facilities.

Methods

Production of the recombinant G117H mutant of human BChE, purification and crystallization. The crystallizable, low-glycosylated, monomeric form of human BChE was mutated into G117H [16], produced in CHO cells, and purified under conditions similar to those described for the wild-type enzyme [23]. Crystals of G117H were prepared in five ways. First, crystals of G117H were grown in an ammonium sulfate containing mother liquor as previously reported, using the hanging-drop vapor-diffusion method, at room temperature [23]. Second, crystals were grown in the mother liquor plus 5 mM $MgCl_2$ and 10 mM NaF as additives. The purpose for this crystallization condition was to generate crystals wherein MgF_3^- would appear as a mimic for PO_3^- in the active site of G117H. Third, crystals were grown in the presence of 5 mM $Al(NO_3)_3$ and 10 mM NaF for the purpose of generating crystals with AlF_4^- in the active site, again as a mimic for PO_3^-. Fourth and fifth, crystals of the VX-G117H and echothiophate-G117H phosphylated enzyme transient adducts were prepared by flash-soaking the G117H crystals for 2 min in 0.1 M MES buffer, pH 6.5, 6% glycerol, 2.1 M ammonium sulfate containing either 1 mM VX or 1 mM echothiophate. The crystals were then washed with a cryoprotectant solution [0.1 M MES buffer pH 6.5 with 2.1 M ammonium sulfate, containing 20% glycerol] and flash-cooled in liquid nitrogen. At this stage, the VX-adduct in the crystals of VX-G117H BChE presents absolutely no danger.

X-ray Data Collection and Structure Solution. Diffraction data for G117H 1) without additives, 2) with $MgCl_2$ and NaF, 3) with $Al(NO_3)_3$ and NaF, or 4) after formation of the echothiophate-G117H adduct were collected at the European Synchrotron Radiation Facility (ESRF, Grenoble), on the ID14-2 beam line using a wavelength of 0.933 Å and an ADSC Quantum 4 detector. Diffraction data for the VX-G117H adduct were collected at the ESRF on the ID23-2 beam line using a wavelength of 0.873 Å and a MAR-Research charge-coupled detector. All data sets were processed with XDS [24] . The structures were solved using the CCP4 suite [25]. An initial model was determined by molecular replacement with MolRep [26], starting with the recombinant BChE structure (PDB entry 1P0I) from which all ligands and glycan chains were removed. For all diffraction data sets, the model was refined as follows: an initial rigid-body refinement was made with REFMAC5 [27], which was followed by iterative cycles of model building with Coot [28]. Finally, restrained and TLS refinements were carried out with REFMAC5. The bound ligands and their descriptions were built using the Dundee PRODRG2.5 server, including energy minimization using GROMOS96.1 force field. Significant drops in R-factor and R-free occurred during the TLS refinement. TLS groups were defined with the help of the *TLS Motion Determination* server (http://skuld.bmsc.washington.edu/~tlsmd/index.html) [29]. The refined TLS parameters are included in the deposited PDB file for each entry. SA-composite omit maps were calculated using Phenix [30] in order to check for any bias in the model. Protein structures were displayed using the program PyMOL (http://www.pymol.org).

Accepted Manuscript

Licenced copy. Copying is not permitted, except with prior permission and as allowed by law.
© 2010 The Authors Journal compilation © 2010 Portland Press Limited

Biochemical Journal Immediate Publication. Published on 19 Nov 2010 as manuscript BJ20101648

THIS IS NOT THE VERSION OF RECORD - see doi:10.1042/BJ20101648

Results

Crystallographic structure of G117H without additives. Crystals were grown in the absence of any extra additives, using ammonium sulfate as a precipitant. Data were collected from tetragonal crystals of space group *I*422 and refined to 2.1 Å. The space group is identical to that formed by the wild-type enzyme. Data and refinement statistics are summarized in Table 1. The mutation does not induce any noticeable conformational change in the enzyme as shown by the marginal all-atoms root mean square deviation of 0.205 Å between G117H BChE and the wild-type BChE (pdb entry 1P0I). In particular, the main chain atoms of Gly117 in the wild type enzyme and of His117 in the mutant enzyme superimpose very well (RMSD=0.225 Å).

Unexpectedly, there is a sulfate ion bound in the active site, opportunely mimicking an organophosphate about to be attacked by the catalytic serine (Fig 1A). The sulfur atom of the sulfate ion is 2.8 Å from Ser198-Oγ; the O1 and S atoms of SO_4^{2-} and the Ser198-Oγ are collinear (175°); and the distance between O1 and Ser198-Oγ is 4.3 Å which compares favorably to the distance between the oxygens located at the apical vertices of a trigonal-bipyramidal phosphorous transition state (4.1 Å). However, the $2|Fo|-|Fc|$ map does not reveal any continuity of electron density between S and Ser198-Oγ. Such continuity would have suggested a covalent bond between these atoms. O4 of the SO_4^{2-} is well stabilized in the oxyanion hole, being at hydrogen-bond distance from the main chain nitrogens of Ala199, Gly116 and His117 (2.9, 3.0 and 2.9 Å, respectively). O3 is stabilized by a strong hydrogen bond with Ser198-Oγ (2.6 Å) and a salt bridge with His117-Nδ1 (2.5 Å). A salt bridge between O2 and His438-Nε2 (2.6 Å) further stabilizes the sulfate ion. His117 adopts a conformation that is not standard (c1=-116°, c2=44°) according to the penultimate rotamer library [31]. This adjustment probably results from the interaction of His117-Nε2 with the main chain carbonyl oxygen of Leu286 (2.8 Å), and from a salt bridge between His117-Nδ1 and the O3 atom of the sulfate (2.5 Å). This conformation is probably not representative of that adopted by His117 in the absence of the sulfate ion, though it could indicate the conformation in the OP complex just prior to phosphorylation of the Ser198.

As is often observed in the crystal structures of wild type BChE [32-35], there is an unidentified ligand stacked against Trp82 that we chose to model by dummy atoms. This ligand is at hydrogen bond distance to O2 of SO_4^{2-} (2.9 Å). In addition, O1 is at hydrogen-bond distance (2.5-3.0 Å) to another unidentified ligand, the electron density of which stretches between Gln119, His117 and Thr120. This density was also modeled by dummy atoms.

Crystallographic structure of G117H in complex with fluoride. Data were collected from tetragonal crystals grown in the presence of $MgCl_2$ and NaF. The original rational for using these additives was to trap a transition state analogue in which MgF_3^- would mimic PO_3^- [36]. This structure was refined to 2.4 Å resolution (See statistics in Table 1).

There are two peaks of electron density in the $|Fo|-|Fc|$ omit maps (green mesh, 4.5 σ). Both are present at the heart of a dense hydrogen bond network involving the oxyanion hole, the catalytic serine (Ser198) and the catalytic histidine (His438) (Fig 1B). One peak likely corresponds to a water molecule which forms one edge of a triangular H-bond network involving Ser198-Oγ and His438-Nε2. The second peak corresponds to an atom that interacts strongly with both the water molecule (2.6 Å) and Ser198-Oγ (2.5 Å), and is at hydrogen bonding distance to the 3 main chain nitrogens of the oxyanion hole residues (Gly116, 3.0 Å; His117, 2.8 Å; Ala199, 2.9 Å). Because the molecule represented by this density was able to displace the sulfate ion that was observed in the absence of NaF, and because there is a three-pronged interaction with the oxyanion hole as expected for a fluoride anion, we modeled this density as a putative fluoride ion.

This interpretation is supported by the fact that the fluoride anion is known to be a reversible inhibitor of BChE [37-39]. Though binding sites have not been identified yet, it is reported that fluoride competes with organophosphates and it was proposed that binding involves two or more hydrogen

Accepted Manuscript

Licenced copy. Copying is not permitted, except with prior permission and as allowed by law.
© 2010 The Authors Journal compilation © 2010 Portland Press Limited

Biochemical Journal Immediate Publication. Published on 19 Nov 2010 as manuscript BJ20101648

donors necessary for enzyme catalysis [40]. Alternatively, a water molecule has been observed in a position similar to that of this putative fluoride ion for some BChE structures [41]. But, the interaction of that water with the oxyanion hole was clearly weaker based on the distance of hydrogen donors, suggesting a two-pronged hydrogen bond interaction.

While the general conformation of His117 in this structure is well resolved, the orientation of the imidazole ring is not. This is because there are two peaks of electron density in the $|Fo|-|Fc|$ maps, one on each side of the imidazole ring suggesting alternate interactions of His117-Nδ1 with 2 water molecules at relatively low occupancy. In the first option, the c1 and c2 angles of His117 are -48° and 103°, respectively (this is the structure shown in Fig 1B). The water molecule (peak at 4.1 σ) is at hydrogen bond distance from the backbone nitrogen of Thr120 (3.1 Å), and interacts strongly with His117-Nδ1 (2.5 Å). In the alternative refined model (position not shown in Fig 1B), the ring is simply flipped with c1=-46° and c2=-71°. The water molecule (peak at 3.5 σ) is at hydrogen bond distance from the carbonyl oxygen of Leu286 (3.1 Å), and interacts very strongly with His117-Nδ1 (2.4 Å). This conformation is reasonably close to the m-70° histidine conformation from the penultimate rotamer library (c1=-65°; c2=-70°) [31]. We favored the first option for the final model of His117 because it better modeled the strongest peak in the $|Fo|-|Fc|$ map and because it kept both water molecules in the structure. The conformation of His117 adopted in Fig 1B is likely to be representative of that found in the mutant structure, in the absence of ligands.

Following the same logic we employed for the $MgCl_2$ and NaF as additives, we grew crystals in the presence of 5 mM $Al(NO_3)_3$ and 10 mM NaF. The idea was to trap an AlF_4^- based transition state analog of PO_3^- in the active site [42]. The crystal structure was refined to 2.4 Å resolution (data not shown). It yielded a crystal structure that was identical to that found when the crystals were grown in the presence of $MgCl_2$ and NaF. This confirmed that fluoride was the key additive leading to the observed complex.

Crystallographic structure of echothiophate-G117H transient adduct. Data were collected from a crystal that was flash-soaked for 2 minutes in a solution containing 1 mM echothiophate. We chose to prepare the crystal in this way because dephosphorylation is partly rate-limiting for the hydrolysis of echothiophate (1.2 min^{-1}) [17]. Therefore, we assumed that the phosphoryl intermediate would likely accumulate in the crystal in the presence of excess echothiophate. The structure was refined to 2.3 Å (See statistics in Table 1).

A strong peak of positive electronic density (11.8 σ), within covalent bond distance of the catalytic serine was seen in the initial $|Fo|-|Fc|$ map (Fig 1C). This is consistent with the presence of a bound diethoxyphosphoryl moiety (DEP). The position of DEP is similar to that which it adopts in wild-type BChE (PDB entry 1XLW) [33]. The phosphorus atom is found at a covalent bonding distance of 1.64 Å from the Ser198-Oγ atom. O3, the phosphoryl oxygen, is at hydrogen bonding distance from the main chain amide nitrogens of the oxyanion hole residues with the shortest distance being to His117N (2.7 Å). There is a very dense hydrogen bond network involving His438-Nε2, Ser198-Oγ, DEP-O2, water molecule 101 and Glu197-Oε1. Given the interatomic distances and angles, the strongest H-bonds are between His438-Nε2 and H_2O-101, and Glu197-Oε1 and H_2O-101 (3.0 Å each).

The H_2O-101 is in the same position as the water molecule 101 described in the DEP conjugate with native BChE (PDB entry 1XLW). This water molecule promotes "aging", i.e. dealkylation of the nearby ethoxy group, by attacking DEP-C3 [33, 43]. Aging via dealkylation was proven by mass spectral analysis of the product after aging in the presence of ^{18}O-water [33, 43].

Comparing DEP-G117H to wild-type DEP-BChE it appears that the His117 side chain induces a concerted shift of DEP-C3 toward H_2O-101 (by 1.2 Å) and H_2O-101 toward Trp82 (by 0.7 Å). As a consequence the distance between DEP-C3 and H_2O-101 is only 2.9 Å in DEP-G117H compared to 3.8 Å in wild-type DEP-BChE. Thus, the imidazole of His117 appears to be an obstacle to the formation of the phosphylated enzyme.

THIS IS NOT THE VERSION OF RECORD - see doi:10.1042/BJ20101648

Accepted Manuscript

Licenced copy. Copying is not permitted, except with prior permission and as allowed by law.
© 2010 The Authors Journal compilation © 2010 Portland Press Limited

BJ Biochemical Journal Immediate Publication. Published on 19 Nov 2010 as manuscript BJ20101648

Given the preeminent role of H_2O-101 in the dealkylation of DEP, it is expected that a shorter distance between DEP-C3 and H_2O-101 would be more favorable for the aging reaction. This was experimentally verified. The dealkylation rate of DEP-G117H is about 7 times faster than that for wild-type DEP-BChE, under similar conditions [17].

His117 also induces a slight rearrangement of the second ethoxy group of DEP and its environment. The imidazole ring prevents DEP-C2 from pointing toward Val288, and thus DEP-C2 is forced toward Leu286. In response, Leu286-Cδ1 and Leu286-Cδ2 shift away by about 1 Å. A similar rearrangement of Leu286 was previously observed in an N-diethylphosphoramidyl conjugate of BChE [35].

His117 adopts a stable conformation (c1=-62°; c2=-76°) corresponding to m-70° from the penultimate rotamer library. The imidazole ring is lying flat, above the diethoxyphosphoryl moiety. This conformation is stabilized by a hydrogen bond between His117-Nε2 and the Pro285-carbonyl-O, and a hydrogen bond to a water molecule bridging His117-Nδ1, and Thr120-Oγ1.

The distances between His117 and the phosphorus of DEP provide some basis on which to address the mechanism of dephosphorylation for DEP-G117H. His117-Nδ1 is 4.6 Å from DEP-P and 3.9 Å from DEP-C3 (respectively 1.3 and 0.6 Å channel width). These distances are too short to allow a water molecule to fit between His117 and the phosphorus as depicted on scheme 2 (pathway B, "attack is anti"). For this path to be active, a conformation change of His117 would have to occur. Alternatively, because His117-Nδ1, DEP-P and Ser198-Oγ are almost collinear (168°), a simple rotation of the imidazole ring by -60° around Cβ-Cγ would place Nδ1 of His117 3.7 Å from DEP-P with the nitrogen lone pair pointing toward the phosphorus atom. This situation seems plausible for a nucleophilic attack of His117 on the phosphorus, i.e. the "Nucleophile is His117" path as depicted in scheme 2 (pathway A).

Crystallographic structure of VX-G117H transient adduct. Data were collected from a crystal that was flash-soaked for 2 minutes in a solution containing 1 mM VX. The reasons for preparing the crystal in this way are the same as those described in the section on the "Crystallographic structure of echothiophate-G117H transient adduct". Because the dephosphonylation rate of VX-G117H is 200 fold lower than that of diethylphosphoryl-G117H, trapping the hydrolysis intermediate was expected to be less challenging. The structure was refined to 2.7 Å (see statistics in Table 1).

No water molecule equivalent to H_2O-101 is present in the active site of the VX-adduct structure (Fig 1D). A peak of electron density more than 4 Å away from His438 and Glu197 was modeled as an ammonium ion likely to be electrostatically interacting with Glu197 and the π system of Trp82 (data not shown).

A peak in the initial $|Fo|-|Fc|$ map (3.7 σ) was found at a covalent bonding distance to Ser198-Oγ (1.7 Å). The absolute configuration of the phosphorous atom is P(S). The methyl group is pointing toward His438 (Fig 1D). The ethoxy group is located in the acyl-binding pocket defined by residues Leu286, Val288 and Trp231. This orientation is the mirror image of that observed in VX-*Tc*AChE [44], but identical to that observed in VX-BChE (Wandhammer et al, submitted).

The ethoxy group points toward Val288, and superimposes very well on the equivalent ethoxy in the wild-type DEP-BChE structure. However, this orientation is different from that just described for the DEP-G117H structure where the ethoxy group was pointing toward Leu286. As a consequence, the shift of Leu286 that is observed in the DEP-G117H conjugate does not occur in the VX-G117H conjugate. And, the carbonyl oxygen from Pro285 is not available for interaction with His117-Nε2. This is reflected in two conformations for His117, which differ by the ring orientation: c1=-7° and c2=-124° or c1=-7° and c2=57°. These conformations are far from common histidine rotamers. This unusual conformational arrangement may be a consequence of the asymmetry of the adduct. That is, the His117 imidazole ring is shifted over the methyl substituent and away from the bulkier ethoxy. In this position, it cannot be stabilized by H-bonding because it is too far from the acceptors in the acyl-binding pocket, and too close to Thr120 to let a bridging water molecule slip in. This translates into much higher

THIS IS NOT THE VERSION OF RECORD - see doi:10.1042/BJ20101648

Accepted Manuscript

Licenced copy. Copying is not permitted, except with prior permission and as allowed by law.
© 2010 The Authors Journal compilation © 2010 Portland Press Limited

Biochemical Journal Immediate Publication. Published on 19 Nov 2010 as manuscript BJ20101648

residual B-factors for the imidazole ring atoms (≈53 Å^3) in comparison to main chain atoms (≈38 Å^3). The corresponding B-factors are much smaller for DEP-G117H, where they are 16 Å^3 for Ca, and 10 Å^3 for His117-Nε2. The large B-factors for the imidazole of His117 in VX-G117H do not permit the orientation of the imidazole ring to be determined with confidence.

Much like in the DEP-G117H structure, His117-Nδ1 is at 4.5 Å from DEP-P and 3.8 Å from DEP-C3. These short distances would not allow a water molecule to get between the phosphorus and His117 in the absence of a large conformational change. His117-Nδ1, DEP-P and Ser198-Oγ are less collinear (157°) than in the DEP-G117H conjugate. Cβ for His117 in VX-G117H is offset by 0.7 Å from its position in DEP-G117H (Fig 2). Thus, the maximum allowable side chain rotation around Cβ-Cγ is -50°. That would partially orient the lone electron pair of His117-Nδ1 toward the adduct, but any further motion toward the phosphorus atom would lead to a clash between His117-Nδ1/Cε2 and the methyl substituent of the VX. This situation is less favorable for a nucleophilic attack of His117 on the phosphorus than was the case in the DEP-G117H intermediate.

THIS IS NOT THE VERSION OF RECORD - see doi:10.1042/BJ20101648

Accepted Manuscript

Licenced copy. Copying is not permitted, except with prior permission and as allowed by law.
© 2010 The Authors Journal compilation © 2010 Portland Press Limited

Biochemical Journal Immediate Publication. Published on 19 Nov 2010 as manuscript BJ20101648

Discussion

Impact of mutations at position 117 on the activity of BChE and related enzymes. When BChE is mutated at position G117 it loses catalytic efficiency for the hydrolysis of thio- and oxo-esters [15, 16]. It was hypothesized that this loss in activity was related to a change in the orientation of the H117 nitrogen proton donor of the oxyanion hole, leading to weaker transition state stabilization due to suboptimal H-bonding [45]. We observe no such change in the X-ray structures of G117H presented here (Figure 2). Though there is some heterogeneity in the positions adopted by His117, depending on the adduct, the positions of the critical oxyanion hole residues are unchanged.

Alternatively, loss of activity toward the normal thio- oxo-esters may be due to the imidazole ring of His117 blocking the approach of substrate and water. This suggestion is based on the fluoride-G117H structure, which we take to be representative of the unliganded, resting enzyme. In this structure, His117 clutters access to the oxyanion hole (Fig 2B), and is very likely a steric obstruction to the formation of all substrate complexes, including the transition state. A change in the position of His117 would be necessary in order to properly orient a substrate in the oxyanion hole, even then optimal orientation may not be achieved.

Such a conformational change is seen in the sulfate complex. If His117 were to maintain the position observed in the fluoride complex, it would collide with the sulfate oxygen that is opposite to the serine. Consequently, the histidine is forced sideways in the sulfate complex.

Similarly, proper fitting of an OP into the active site of BChE requires a conformational change of His117 (compare Fig 1A to Fig 1C and Fig 1D). Such steric hindrance from His117 could explain the 2- to 4-order of magnitude decrease in phosphylation rates observed for OPs reacting with G117H [46].

Loss of sensitivity to organophosphate inhibitors in insects may be attributed to the same phenomenon. For example, a natural mutation in mosquito acetylcholinesterase, G119S – a position equivalent of G117 in BChE – is at the origin of their resistance to organophosphate pesticides [47]. No OP hydrolase activity was reported for this mutant, but resistance could arise from decreased affinity for OP. It is noteworthy to mention that no OP-hydrolase activity was observed for the equivalent BChE mutant, G117S [20]. A second example is the G137D mutant of carboxylesterase from the sheep blowfly [48]. Position 137 is equivalent to position 117 in BChE and substitution of Asp for Gly at this position would be expected to hinder access to the oxyanion hole. The G137D mutation reduces sensitivity to OPs and confers OP-hydrolase activity on the carboxylesterase. OP-hydrolase activity was also found for the equivalent G117D mutation in BChE [20]. Finally, a triple mutation in *Bungarus fasciatus* AChE aimed at introducing a histidine into a position homologous to 117 of BChE reduces sensitivity to OPs and turns this enzyme into an OP hydrolase [49].

Candidate mechanisms for catalytic dephosphylation. Four different mechanisms have been proposed by previous investigators to explain why dephosphylation of G117H BChE is faster than dephosphylation of the native enzyme (Scheme 2).

Mechanism A

The first mechanism is based on a nucleophilic attack of His117 on the phosphorus, leading to a phosphylhistidine intermediate that is subsequently hydrolyzed (Scheme 2 pathway A, the "Nucleophile is His117" pathway). This mechanism was originally proposed by Fortier on the basis of molecular mechanics calculations [50].

One argument against this mechanism is that phosphohistidines have a high-energy phosphoramidate bond and tend to transfer the phosphoryl group to other molecules [51, 52]. Thus it would be expected that a phosphylhistidine would transfer its phosphyl moiety to the serine and not the other way around. Following this reasoning, early investigators proposed that the OP-serine adduct was formed via an intermediate OP-histidine donor rather than through a direct phosphylation by the OP [53].

THIS IS NOT THE VERSION OF RECORD - see doi:10.1042/BJ20101648

Accepted Manuscript

Licenced copy. Copying is not permitted, except with prior permission and as allowed by law.
© 2010 The Authors Journal compilation © 2010 Portland Press Limited

Biochemical Journal Immediate Publication. Published on 19 Nov 2010 as manuscript BJ20101648

Support for nucleophilic attack by His117 on the phosphorus comes from the colinearity of His117-Nδ1, the phosphorus atom and Ser198-Oγ in the DEP-G117H conjugate, and to a lesser extent in the VX-G117H conjugate. A 60° rotation of the imidazole ring around the Cβ-Cγ bond would orient the lone pair of electrons on the nitrogen toward the phosphorus for direct nucleophilic attack. Unfortunately, the phosphorus substituents are in close contact with the imidazole ring and these interactions would prevent a simple rotation around Cβ-Cγ bond. Rotation could occur only if His117 moved back from the phosphorus substantially. Even if the simple rotation were to occur, the imidazole would still be 3.7 Å from the phosphorus, too far for covalent interaction. Taken together, the crystal data and the thermodynamics argue that pathway A is unlikely. Proof for this mechanism would require trapping of the phosphylhistidine intermediate.

Mechanism B

The second mechanism is a nucleophilic attack by water on the phosphorus atom, promoted by His117. The oxygen of the attacking water would have to be positioned opposite the serine–phosphorus bond, i.e. in an apical or "anti" position (Scheme 2, pathway B, "attack is anti"). This mechanism formed the basis of the original rationale for the design of the G117H mutant [54]. Broomfield and Millard reasoned that "it might be possible to introduce a second nucleophilic center into the active site in such a position that it could carry an activated water molecule to the face of the phosphorus moiety opposite the phosphorus-serine bond and thereby reactivate the enzyme" [54]. Newcomb et al. extended this mechanism to the G137D mutant of the sheep blowfly carboxylesterase, the aspartate acting as a base to orientate a water molecule in the appropriate position for hydrolysis [48]. By analogy, this mechanism was also proposed for the G117D, G117E, and L286H BChE mutants [20]. Finally, this mechanism was recently re-proposed by Amitay et al. based on similarities with RNase A [21]. The active site of RNase A contains two histidine residues, His12 and His119, in locations comparable to His117 and His438 of BChE. His12 serves as a base to abstract a proton from the 2'-oxygen of the RNA substrate molecule, thereby activating it for attack on the phosphorus. His119 serves as an acid to protonate the oxygen of the leaving group [55].

The X-ray structures in Figures 1C and 1D show that the imidazole of His117 is in close contact with the phosphorus. In this position His117 would not allow a water molecule to approach the phosphorus. A large conformational change of His117 would be required to make room. In addition, if one considers the sulfate-G117H complex to be a structural analog of the dephosphylation transition state for mechanism B, then the formation of the transition state is obstructed by the ethoxy moiety in the acyl-binding pocket as seen by the superimposition of the sulfate, VX and DEP-G117H (Figure 2). Finally, the imidazole of His117 is an obstacle to the formation of the dephosphylation transition state, much like it is an obstacle for the formation of the phosphylation transition state in agreement with kinetic data [16]. These observations argue that a conformational change in the active center would be necessary for Mechanism B to occur. A partially rate limiting conformational change in course of forming the transition state for dephosphylation is consistent with the weak pH dependencies observed for dephosphylation [16, 17]. QM/MM calculations based on the structures herein would be needed in order to determine if the change of conformation required corresponds to an energy barrier compatible with the measured dephosphylation rate.

Mechanism C

The third mechanism, which was proposed by Millard et al. [16], derives from the suggestion of Kovach that the dephosphylation rate is inversely proportional to the electron density on the phosphorus [56]. Millard proposed that a hydrogen bond between His438 and an alkoxy ligand to the phosphorus stabilized the linkage between the phosphorus and Ser198-Oγ by making His438 unavailable to serve in its traditional role of transferring a proton to Ser198. It was proposed that His117 would compete with His438 by forming a hydrogen bond with the one of the ethoxy groups thus setting His438 free to form a hydrogen bond with a water molecule. Abstraction of a proton from that water molecule, would

THIS IS NOT THE VERSION OF RECORD - see doi:10.1042/BJ20101648

Accepted Manuscript

Licenced copy. Copying is not permitted, except with prior permission and as allowed by law.
© 2010 The Authors Journal compilation © 2010 Portland Press Limited

Biochemical Journal Immediate Publication. Published on 19 Nov 2010 as manuscript BJ20101648

promote attack of the water on the phosphorus atom. The structure of VX-G117H (Fig 1D) shows no hydrogen bonding interactions for the imidazole of His117 with the ethoxy substituents. The structure of DEP-G117H (Fig 1C) shows His117 making H-bond contact with water molecules but not with the ethoxy substituent. In the DEP-G117H complex His438 is at an optimal position to transfer a proton between a water molecule and the serine while maintaining a hydrogen bond to an ethoxy group. These observations refute the idea that H-bonding of His438 to an ethoxy group is a critical feature of phosphylated G117H that would prevent it from acting as a base catalyst.

Mechanism D

The structure in Fig 1C supports a mechanism in which a water molecule could be activated by His438 for attack on the phosphorus atom. His438 in DEP-G117H is hydrogen bonded to a water located near the wide-open face of the DEP adduct, adjacent to Ser198 (Scheme 2, pathway C). If His438 is deprotonated then it could abstract a proton from the entering water molecule and subsequently transfer it to the serine. Alternatively, if it is protonated then it could serve as a relay in a concerted proton transfer from the water molecule to the catalytic serine as depicted in scheme 2, pathway C. A similar adjacent nucleophilic substitution mechanism has been proposed in some phosphylation and aging reactions of cholinesterases [57, 58].

H-bonding of the water to Glu197 that is seen in Fig 1C can further stabilize the approaching water molecule. A role for Glu197 in dephosphylation is supported by the observation that there is 40-fold decrease in the dephosphorylation rate of echothiophate-G117H/E197Q [20], but a 10-fold increase in the dephosphonylation rate for VX- and sarin-G117H/E197Q mutants [18].

In Mechanism D, His117 could accelerate dephosphylation by destabilizing the transient phosphylserine by steric obstruction. Indeed, the conformation of His117 in the DEP- and methylethoxyphosphonyl-G117H transient conjugates, appears to be strained by comparison to the relaxed conformation observed in the fluoride-G117H complex (Figure 2). The imidazole ring puts a lot of strain on the phosphyl moiety and can be viewed as a molecular analog of a loaded spring. This should result in a high-energy structure, destabilizing the adduct. The destabilizing role of His117 in the transition state would therefore be simply steric exclusion. Given this thesis, a diethylphosphoryl adduct is expected to be under greater strain than a methylethoxyphosphonyl adduct, thus explaining the higher hydrolysis rate for echothiophate than for VX. Additionally, if His117 is charged, it is expected to enhance the electrophily of the phosphorus atom by a local electrostatic effect. These effects would also be consistent with the modest pH dependence on the dephosphylation step [16, 17]. All things considered, mechanism D appears to be most consistent with the X-ray data.

In summary, the structures presented here are not sufficient to definitively identify the molecular mechanism of G117H phosphyl hydrolysis, however they do provide a basis on which to question the currently advanced possibilities. In addition, the X-ray structures of echothiophate-G117H and VX-G117H provide indispensable structural templates for future QM/MM calculations and valuable structural starting points for further explorations into the hydrolysis mechanism. The proposals provided in this discussion also may provide guidance for computational mutagenesis directed at improving the dephosphylation rates for G117H. A mutagenesis strategy based on computational design was successfully implemented to create a mutant of BChE with improved cocaine hydrolase activity [59]. Such a strategy could be applied to the design of new cholinesterases or other serine hydrolase mutants that can more efficiently reactivate from OP inhibition. Efficient catalytic bioscavengers would provide a great improvement in prophylaxis, decontamination and treatment of organophosphylate poisoning.

Acknowledgments. The authors thank Dr S. Lushchekina (Univ. Lomonosov, Moscow, Ru) for fruitful discussions.

THIS IS NOT THE VERSION OF RECORD - see doi:10.1042/BJ20101648

Accepted Manuscript

Licenced copy. Copying is not permitted, except with prior permission and as allowed by law.
© 2010 The Authors Journal compilation © 2010 Portland Press Limited

Biochemical Journal Immediate Publication. Published on 19 Nov 2010 as manuscript BJ20101648

Funding. This work was supported by ANR-06-BLAN-0163 and DGA/PEA 08co501 to FN.

Accepted Manuscript

THIS IS NOT THE VERSION OF RECORD - see doi:10.1042/BJ20101648

Licenced copy. Copying is not permitted, except with prior permission and as allowed by law.
© 2010 The Authors Journal compilation © 2010 Portland Press Limited

Biochemical Journal Immediate Publication. Published on 19 Nov 2010 as manuscript BJ20101648

References

1 Gerlt, J. A. and Babbitt, P. C. (2009) Enzyme (re)design: lessons from natural evolution and computation. Curr. Opin. Chem. Biol. **13**, 10-18

2 Harel, M., Sussman, J. L., Krejci, E., Bon, S., Chanal, P., Massoulie, J. and Silman, I. (1992) Conversion of acetylcholinesterase to butyrylcholinesterase: modeling and mutagenesis. Proc. Natl. Acad. Sci. U. S. A. **89**, 10827-10831

3 Kaplan, D., Ordentlich, A., Barak, D., Ariel, N., Kronman, C., Velan, B. and Shafferman, A. (2001) Does "butyrylization" of acetylcholinesterase through substitution of the six divergent aromatic amino acids in the active center gorge generate an enzyme mimic of butyrylcholinesterase? Biochemistry. **40**, 7433-7445

4 Li, B., Stribley, J. A., Ticu, A., Xie, W., Schopfer, L. M., Hammond, P., Brimijoin, S., Hinrichs, S. H. and Lockridge, O. (2000) Abundant tissue butyrylcholinesterase and its possible function in the acetylcholinesterase knockout mouse. J. Neurochem. **75**, 1320-1331

5 Schopfer, L. M., Furlong, C. E. and Lockridge, O. (2010) Development of diagnostics in the search for an explanation of toxic airline syndrome. Anal. Biochem. **404**, 64-74

6 Lockridge, O. and Masson, P. (2000) Pesticides and susceptible populations: people with butyrylcholinesterase genetic variants may be at risk. Neurotoxicology. **21**, 113-126

7 Masson, P., Carletti, E. and Nachon, F. (2009) Structure, Activities and Biomedical Applications of Human Butyrylcholinesterase. Protein Pept Lett. **16**, 1215-1224

8 Zheng, F., Yang, W., Ko, M. C., Liu, J., Cho, H., Gao, D., Tong, M., Tai, H. H., Woods, J. H. and Zhan, C. G. (2008) Most efficient cocaine hydrolase designed by virtual screening of transition states. J. Am. Chem. Soc. **130**, 12148-12155

9 Heilbronn, E. (1993) Molecular biology of cholinesterases, a background and an introduction. In Cholinergic Function and Dysfunction. (Cuello, A. C., ed.). pp. 133-138, Elsevier, Amsterdam

10 Lenz, D. E., Broomfield, C. A., Yeung, D. T., Masson, P., Maxwell, D. M. and Cerasoli, D. M. (2007) Nerve agent bioscavengers: progress in development of a new mode of protection against organophosphorus exposure. In Chemical Warfare Agents: Chemistry, Pharmacology, Toxicology and Therapeutics (Romano, J. A., Luckey, B. J. and Salem, H., eds.). pp. 145-173, CRC Press, Boca Raton, Fl

11 Huang, Y. J., Huang, Y., Baldassarre, H., Wang, B., Lazaris, A., Leduc, M., Bilodeau, A. S., Bellemare, A., Cote, M., Herskovits, P., Touati, M., Turcotte, C., Valeanu, L., Lemee, N., Wilgus, H., Begin, I., Bhatia, B., Rao, K., Neveu, N., Brochu, E., Pierson, J., Hockley, D. K., Cerasoli, D. M., Lenz, D. E., Karatzas, C. N. and Langermann, S. (2007) Recombinant human butyrylcholinesterase from milk of transgenic animals to protect against organophosphate poisoning. Proc. Natl. Acad. Sci. U. S. A. **104**, 13603-13608

12 Ashani, Y. and Pistinner, S. (2004) Estimation of the upper limit of human butyrylcholinesterase dose required for protection against organophosphates toxicity: a mathematically based toxicokinetic model. Toxicol. Sci. **77**, 358-367

13 Lenz, D. E., Yeung, D., Smith, J. R., Sweeney, R. E., Lumley, L. A. and Cerasoli, D. M. (2007) Stoichiometric and catalytic scavengers as protection against nerve agent toxicity: a mini review. Toxicology. **233**, 31-39

14 Järv, J. (1984) Stereochemical aspects of cholinesterase catalysis. Bioorganic Chemistry. **12**, 259-278

15 Masson, P., Nachon, F., Broomfield, C. A., Lenz, D. E., Verdier, L., Schopfer, L. M. and Lockridge, O. (2008) A collaborative endeavor to design cholinesterase-based catalytic scavengers against toxic organophosphorus esters. Chem. Biol. Interact. **175**, 273-280

THIS IS NOT THE VERSION OF RECORD - see doi:10.1042/BJ20101648

Accepted Manuscript

Licenced copy. Copying is not permitted, except with prior permission and as allowed by law.
© 2010 The Authors Journal compilation © 2010 Portland Press Limited

BJ Biochemical Journal Immediate Publication. Published on 19 Nov 2010 as manuscript BJ20101648

16 Millard, C. B., Lockridge, O. and Broomfield, C. A. (1995) Design and expression of organophosphorus acid anhydride hydrolase activity in human butyrylcholinesterase. Biochemistry. **34**, 15925-15933
17 Lockridge, O., Blong, R. M., Masson, P., Froment, M. T., Millard, C. B. and Broomfield, C. A. (1997) A single amino acid substitution, Gly117His, confers phosphotriesterase (organophosphorus acid anhydride hydrolase) activity on human butyrylcholinesterase. Biochemistry. **36**, 786-795
18 Millard, C. B., Lockridge, O. and Broomfield, C. A. (1998) Organophosphorus acid anhydride hydrolase activity in human butyrylcholinesterase: synergy results in a somanase. Biochemistry. **37**, 237-247
19 Wang, Y., Boeck, A. T., Duysen, E. G., Van Keuren, M., Saunders, T. L. and Lockridge, O. (2004) Resistance to organophosphorus agent toxicity in transgenic mice expressing the G117H mutant of human butyrylcholinesterase. Toxicol. Appl. Pharmacol. **196**, 356-366
20 Schopfer, L. M., Ticu-Boeck, A., Broomfield, C. A. and Lockridge, O. (2004) Mutants of human butyrylcholinesterase with organophosphate hydrolase activity; evidence that His117 serves as a general base catalyst. J. Med. Chem. Def. **2**, 1-21
21 Amitay, M. and Shurki, A. (2009) The structure of G117H mutant of butyrylcholinesterase: Nerve agents scavenger. Proteins. **77**, 370-377
22 Vyas, S., Beck, J. M., Xia, S., Zhang, J. and Hadad, C. M. (2010) Butyrylcholinesterase and G116H, G116S, G117H, G117N, E197Q and G117H/E197Q mutants: A molecular dynamics study. Chem. Biol. Interact. **187**, 241-245
23 Nachon, F., Nicolet, Y., Viguie, N., Masson, P., Fontecilla-Camps, J. C. and Lockridge, O. (2002) Engineering of a monomeric and low-glycosylated form of human butyrylcholinesterase: expression, purification, characterization and crystallization. Eur. J. Biochem. **269**, 630-637
24 Kabsch, W. (2010) Xds. Acta Crystallogr. Sect. D. Biol. Crystallogr. **66**, 125-132
25 CCP4, C. C. P., Number 4). (1994) The CCP4 suite: Programs for Protein Crystallography. Acta Crystallogr. Sect. D. Biol. Crystallogr. **D50**, 760-763
26 Vagin, A. and Teplyakov, A. (1997) MOLREP: an automatedprogram for molecular replacement. J. Appl. Crystallogr. **30**, 1022-1025
27 Murshudov, G. N., Vagin, A. A. and Dodson, E. J. (1997) Refinement of macromolecular structures by the maximum-likelihood method. Acta Crystallogr. Sect. D. Biol. Crystallogr. **53**, 240-255
28 Emsley, P. and Cowtan, K. (2004) Coot: model-building tools for molecular graphics. Acta Crystallogr. Sect. D. Biol. Crystallogr. **60**, 2126-2132
29 Painter, J. and Merritt, E. A. (2006) Optimal description of a protein structure in terms of multiple groups undergoing TLS motion. Acta Crystallogr. Sect. D. Biol. Crystallogr. **62**, 439-450
30 Adams, P. D., Afonine, P. V., Bunkoczi, G., Chen, V. B., Davis, I. W., Echols, N., Headd, J. J., Hung, L. W., Kapral, G. J., Grosse-Kunstleve, R. W., McCoy, A. J., Moriarty, N. W., Oeffner, R., Read, R. J., Richardson, D. C., Richardson, J. S., Terwilliger, T. C. and Zwart, P. H. (2010) PHENIX: a comprehensive Python-based system for macromolecular structure solution. Acta Crystallogr. Sect. D. Biol. Crystallogr. **66**, 213-221
31 Lovell, S. C., Word, J. M., Richardson, J. S. and Richardson, D. C. (2000) The penultimate rotamer library. Proteins. **40**, 389-408
32 Nicolet, Y., Lockridge, O., Masson, P., Fontecilla-Camps, J. C. and Nachon, F. (2003) Crystal structure of human butyrylcholinesterase and of its complexes with substrate and products. J. Biol. Chem. **278**, 41141-41147
33 Nachon, F., Asojo, O. A., Borgstahl, G. E., Masson, P. and Lockridge, O. (2005) Role of water in aging of human butyrylcholinesterase inhibited by echothiophate: the crystal structure suggests two alternative mechanisms of aging. Biochemistry. **44**, 1154-1162

THIS IS NOT THE VERSION OF RECORD - see doi:10.1042/BJ20101648

Accepted Manuscript

Licenced copy. Copying is not permitted, except with prior permission and as allowed by law.
© 2010 The Authors Journal compilation © 2010 Portland Press Limited

BJ Biochemical Journal Immediate Publication. Published on 19 Nov 2010 as manuscript BJ20101648

34 Carletti, E., Li, H., Li, B., Ekstrom, F., Nicolet, Y., Loiodice, M., Gillon, E., Froment, M. T., Lockridge, O., Schopfer, L. M., Masson, P. and Nachon, F. (2008) Aging of cholinesterases phosphylated by tabun proceeds through O-dealkylation. J. Am. Chem. Soc. **130**, 16011-16020

35 Carletti, E., Aurbek, N., Gillon, E., Loiodice, M., Nicolet, Y., Fontecilla-Camps, J. C., Masson, P., Thiermann, H., Nachon, F. and Worek, F. (2009) Structure-activity analysis of aging and reactivation of human butyrylcholinesterase inhibited by analogues of tabun. Biochem. J. **421**, 97-106

36 Baxter, N. J., Olguin, L. F., Golicnik, M., Feng, G., Hounslow, A. M., Bermel, W., Blackburn, G. M., Hollfelder, F., Waltho, J. P. and Williams, N. H. (2006) A Trojan horse transition state analogue generated by MgF3- formation in an enzyme active site. Proc. Natl. Acad. Sci. U. S. A. **103**, 14732-14737

37 Cimasoni, G. (1966) Inhibition of cholinesterases by fluoride in vitro. Biochem. J. **99**, 133-137

38 Page, J. D., Wilson, I. B. and Silman, I. (1985) Butyrylcholinesterase: inhibition by arsenite, fluoride, and other ligands, cooperativity in binding. Mol. Pharmacol. **27**, 437-443

39 Masson, P., Adkins, S., Gouet, P. and Lockridge, O. (1993) Recombinant human butyrylcholinesterase G390V, the fluoride-2 variant, expressed in Chinese hamster ovary cells, is a low affinity variant. J. Biol. Chem. **268**, 14329-14341

40 Ashani, Y., Segev, O. and Balan, A. (2004) The effect of fluoride on the scavenging of organophosphates by human butyrylcholinesterase in buffer solutions and human plasma. Toxicol. Appl. Pharmacol. **194**, 90-99

41 Ngamelue, M. N., Homma, K., Lockridge, O. and Asojo, O. A. (2007) Crystallization and X-ray structure of full-length recombinant human butyrylcholinesterase. Acta Crystallogr. Sect. F Struct. Biol. Cryst. Commun. **63**, 723-727

42 Xu, Y. W., Morera, S., Janin, J. and Cherfils, J. (1997) AlF3 mimics the transition state of protein phosphorylation in the crystal structure of nucleoside diphosphate kinase and MgADP. Proc. Natl. Acad. Sci. U. S. A. **94**, 3579-3583

43 Li, H., Schopfer, L. M., Nachon, F., Froment, M. T., Masson, P. and Lockridge, O. (2007) Aging pathways for organophosphate-inhibited human butyrylcholinesterase, including novel pathways for isomalathion, resolved by mass spectrometry. Toxicol. Sci. **100**, 136-145

44 Millard, C. B., Koellner, G., Ordentlich, A., Shafferman, A., Silman, I. and Sussman, J. L. (1999) Reaction Products of Acetylcholinesterase and VX Reveal a Mobile Histidine in the Catalytic Triad. J. Am. Chem. Soc. **121**, 9883- 9884

45 Masson, P., Froment, M. T., Gillon, E., Nachon, F., Lockridge, O. and Schopfer, L. M. (2007) Hydrolysis of oxo- and thio-esters by human butyrylcholinesterase. Biochim. Biophys. Acta. **1774**, 16-34

46 Broomfield, C. A., Lockridge, O. and Millard, C. B. (1999) Protein engineering of a human enzyme that hydrolyzes V and G nerve agents: design, construction and characterization. Chem. Biol. Interact. **119-120**, 413-418

47 Weill, M., Lutfalla, G., Mogensen, K., Chandre, F., Berthomieu, A., Berticat, C., Pasteur, N., Philips, A., Fort, P. and Raymond, M. (2003) Comparative genomics: Insecticide resistance in mosquito vectors. Nature. **423**, 136-137

48 Newcomb, R. D., Campbell, P. M., Ollis, D. L., Cheah, E., Russell, R. J. and Oakeshott, J. G. (1997) A single amino acid substitution converts a carboxylesterase to an organophosphorus hydrolase and confers insecticide resistance on a blowfly. Proc. Natl. Acad. Sci. U. S. A. **94**, 7464-7468

49 Poyot, T., Nachon, F., Froment, M. T., Loiodice, M., Wieseler, S., Schopfer, L. M., Lockridge, O. and Masson, P. (2006) Mutant of Bungarus fasciatus acetylcholinesterase with low affinity and low hydrolase activity toward organophosphorus esters. Biochim. Biophys. Acta. **1764**, 1470-1478

50 Albaret, C., Masson, P., Broomfield, C. A., El Kaim, L. and Fortier, P. L. (1998) Mechanical aspects of the phosphotriesterase activity of human butyrylcholinesterase G117H mutant. In

THIS IS NOT THE VERSION OF RECORD - see doi:10.1042/BJ20101648

Accepted Manuscript

Licenced copy. Copying is not permitted, except with prior permission and as allowed by law.

© 2010 The Authors Journal compilation © 2010 Portland Press Limited

Biochemical Journal Immediate Publication. Published on 19 Nov 2010 as manuscript BJ20101648

Structure and Function of cholinesterases and related proteins (Doctor, B. P., ed.). pp. 399-405, Plenum Press, New York, NY

51 Stock, J. B., Stock, A. M. and Mottonen, J. M. (1990) Signal transduction in bacteria. Nature. **344**, 395-400

52 Attwood, P. V., Piggott, M. J., Zu, X. L. and Besant, P. G. (2007) Focus on phosphohistidine. Amino Acids. **32**, 145-156

53 Hobbiger, F. (1955) Effect of nicotinhydroxamic acid methiodide on human plasma cholinesterase inhibited by organophosphates containing a dialkylphosphato group. Br J Pharmacol Chemother. **10**, 356-362

54 Broomfield, C. A., Millard, C. B., Lockridge, O. and Caviston, T. L. (1995) In Enzymes of the Cholinesterase Family (Quinn, D. M., Balasubramanian, A. S., Doctor, B. P. and Taylor, P., eds.). pp. 169-175, Plenum Press, New York

55 Raines, R. T. (1998) Ribonuclease A. Chem. Rev. **98**, 1045-1066

56 Kovach, I. M. (1988) Structure and dynamics of serine hydrolase-organophosphate adducts. J Enzyme Inhib. **2**, 199-208

57 Kwasnieski, O., Verdier, L., Malacria, M. and Derat, E. (2009) Fixation of the two Tabun isomers in acetylcholinesterase: a QM/MM study. J Phys Chem B. **113**, 10001-10007

58 Nachon, F., Carletti, E., Worek, F. and Masson, P. (2010) Aging mechanism of butyrylcholinesterase inhibited by an N-methyl analogue of tabun: Implications of the trigonal-bipyramidal transition state rearrangement for the phosphylation or reactivation of cholinesterases. Chem. Biol. Interact. **187**, 44-48

59 Zhan, C. G., Zheng, F. and Landry, D. W. (2003) Fundamental reaction mechanism for cocaine hydrolysis in human butyrylcholinesterase. J. Am. Chem. Soc. **125**, 2462-2474

THIS IS NOT THE VERSION OF RECORD - see doi:10.1042/BJ20101648

Accepted Manuscript

Licenced copy. Copying is not permitted, except with prior permission and as allowed by law.

© 2010 The Authors Journal compilation © 2010 Portland Press Limited

Biochemical Journal Immediate Publication. Published on 19 Nov 2010 as manuscript BJ20101648

Table

Table 1: Data Collection and Refinement Statistics				
Ligand PDB entry code	Sulfate 2xmb	Fluoride 2xmc	Echothiophate 2xmd	VX 2xmg
Data				
ESRF Beamline	ID14-2	ID14-1	ID14-2	ID23-2
space group	I422	I422	I422	I422
unit cell axes, *a*=*b*, *c* (Å)	154.8, 134.6	155.6, 128.0	154.9, 127.5	156.6, 128.4
no. of measured reflections	308251	154794	249541	166904
unique reflections	47525	29897	33216	20940
resolution (Å)	37.6-2.1(2.4-2.1)	41.1-2.4(2.5-2.4)	28.1-2.3(2.4-2.3)	55.5-2.7(2.8-2.7)
completeness (%)	99.5(99.0)	96.7(96.2)	95.9(85.4)	94.3(95.0)
*R*sym (%)	6.1(36.4)	5.6(51.0)	4.9(23.9)	7.1(56.0)
I/σ(I)	21.3(5.7)	28.0(3.6)	28.9(6.0)	23.7(3.8)
Redundancy	6.4(6.5)	5.1(4.9)	7.5(4.5)	8.0(7.4)
Refinement Statistics				
R-factor[a] (*R*-free[b])	16.8(20.8)	19.2(25.2)	17.0(21.4)	17.6(25.0)
no. of atoms				
protein	4209	4216	4226	4226
solvent	380	229	285	151
others	189	171	198	168
mean *B*-factor (Å^2)	41.7	46.08	40.08	56.14
RMS from ideality				
bond length (Å)	0.024	0.021	0.023	0.018
angles (deg)	2.182	2.009	2.090	1.933
chiral (Å^3)	0.154	0.140	0.157	0.128

[a] R-factor=Σ |Fo - |Fc|| / Σ |Fo|, Fo and Fc are observed and calculated structure factors
[b] R-free set uses about 1000 randomly chosen reflections.

THIS IS NOT THE VERSION OF RECORD - see doi:10.1042/BJ20101648

Accepted Manuscript

Licenced copy. Copying is not permitted, except with prior permission and as allowed by law.
© 2010 The Authors Journal compilation © 2010 Portland Press Limited

Biochemical Journal Immediate Publication. Published on 19 Nov 2010 as manuscript BJ20101648

Figure legends

Scheme 1: Chemical structures of VX and echothiophate. The asterisk denotes a chiral center.

Scheme 2: Potential mechanisms for the hydrolysis of echothiophate by G117H. The Upper pathway (A) involves the nucleophilic attack by His117 on the phosphorus of the adduct followed by the hydrolysis of the phosphylhistidine by a water molecule. The lower pathways involve a nucleophilic attack by a water molecule on the phosphorus of the adduct, either from a position anti (B) or adjacent (C and D) to the catalytic serine.

Figure 1: The active site of G117H BChE: (A) in the presence of sulfate; (B) in the presence of fluoride; (C) with diethylphosphate covalently attached to Ser198, i.e an echothiophate adduct; and (D) with O-ethyl-methylphosphonate attached to Ser198, i.e. a VX adduct. Active site residues are shown in the ball-and-sticks format. Carbon atoms are shown in bright orange (or cyan for key residues), nitrogen atoms in deep blue, the phosphorus atom in orange, and oxygen atoms in red. Hydrogen bonds are represented by dashes. The electron density $|Fo|-|Fc|$ omit map is represented by a green mesh contoured at 3σ.

Figure 2: Two views of the active site of butyryl-BChE (blue, PDB code 1p0i) superimposed on the G117H complex with sulfate (orange), fluoride (cyan), echothiophate (green) and VX (red). Side (A) and front (B)

THIS IS NOT THE VERSION OF RECORD - see doi:10.1042/BJ20101648

Accepted Manuscript

Licenced copy. Copying is not permitted, except with prior permission and as allowed by law.
© 2010 The Authors Journal compilation © 2010 Portland Press Limited

Biochemical Journal Immediate Publication. Published on 19 Nov 2010 as manuscript BJ20101648

Scheme 1

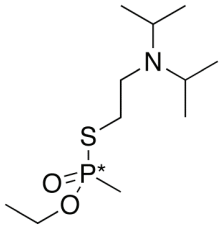

VX

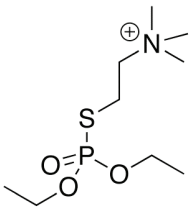

Echothiophate

THIS IS NOT THE VERSION OF RECORD - see doi:10.1042/BJ20101648

Accepted Manuscript

Licenced copy. Copying is not permitted, except with prior permission and as allowed by law.
© 2010 The Authors Journal compilation © 2010 Portland Press Limited

Biochemical Journal Immediate Publication. Published on 19 Nov 2010 as manuscript BJ20101648

Scheme 2

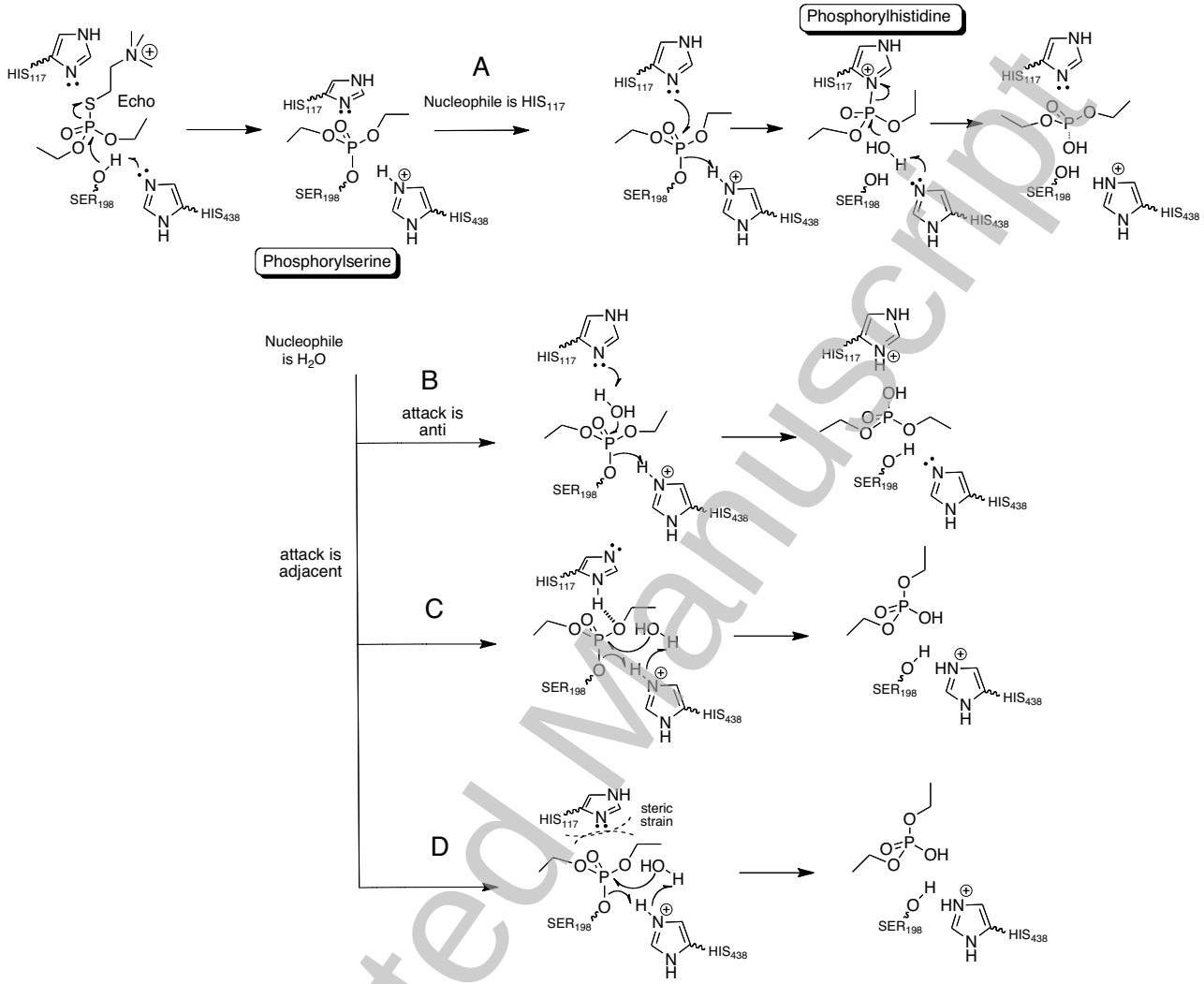

THIS IS NOT THE VERSION OF RECORD - see doi:10.1042/BJ20101648

Accepted Manuscript

Licenced copy. Copying is not permitted, except with prior permission and as allowed by law.
© 2010 The Authors Journal compilation © 2010 Portland Press Limited

Biochemical Journal Immediate Publication. Published on 19 Nov 2010 as manuscript BJ20101648

Figure 1

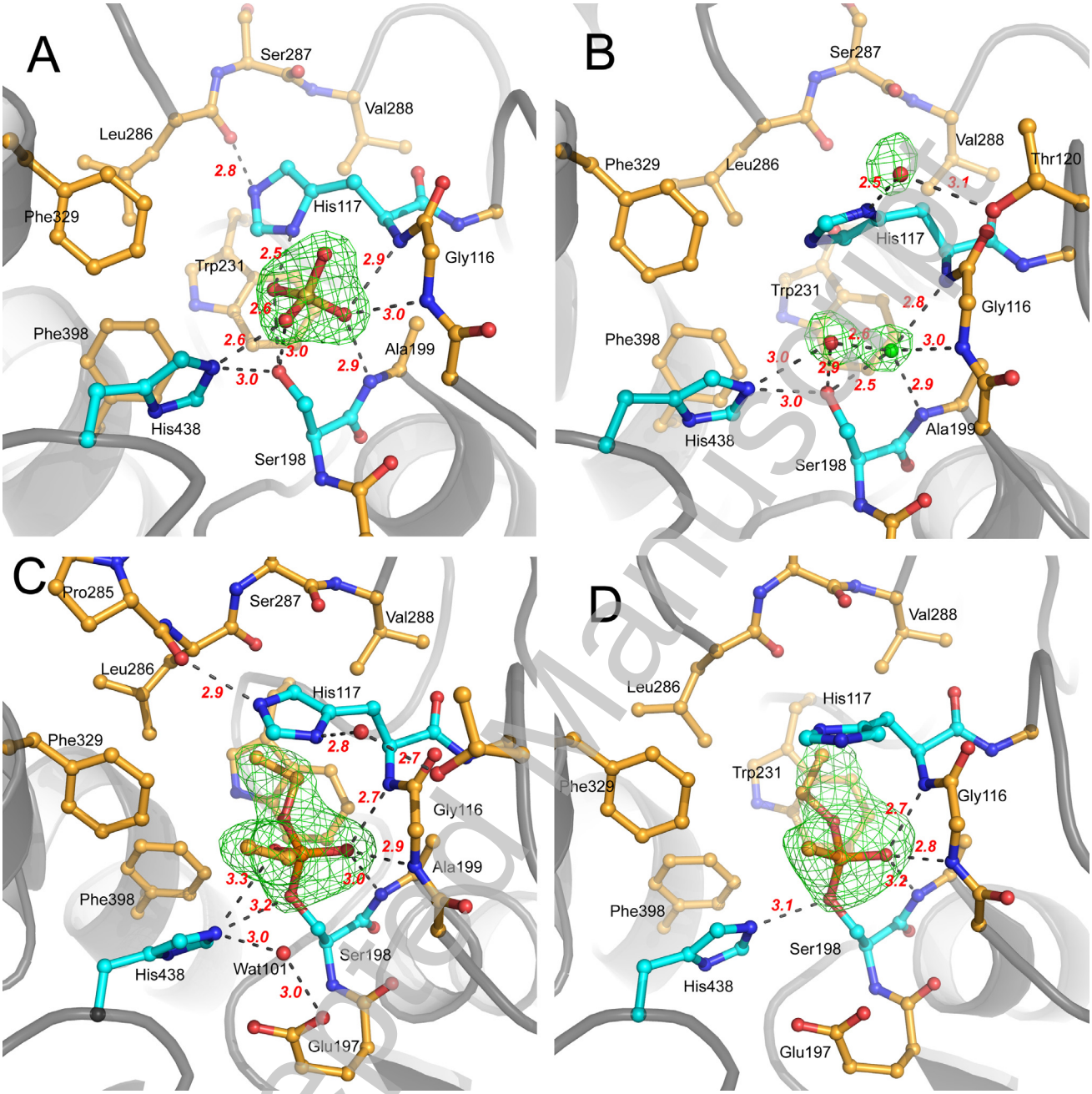

THIS IS NOT THE VERSION OF RECORD - see doi:10.1042/BJ20101648

Accepted Manuscript

Licenced copy. Copying is not permitted, except with prior permission and as allowed by law.
© 2010 The Authors Journal compilation © 2010 Portland Press Limited

Biochemical Journal Immediate Publication. Published on 19 Nov 2010 as manuscript BJ20101648

Figure 2

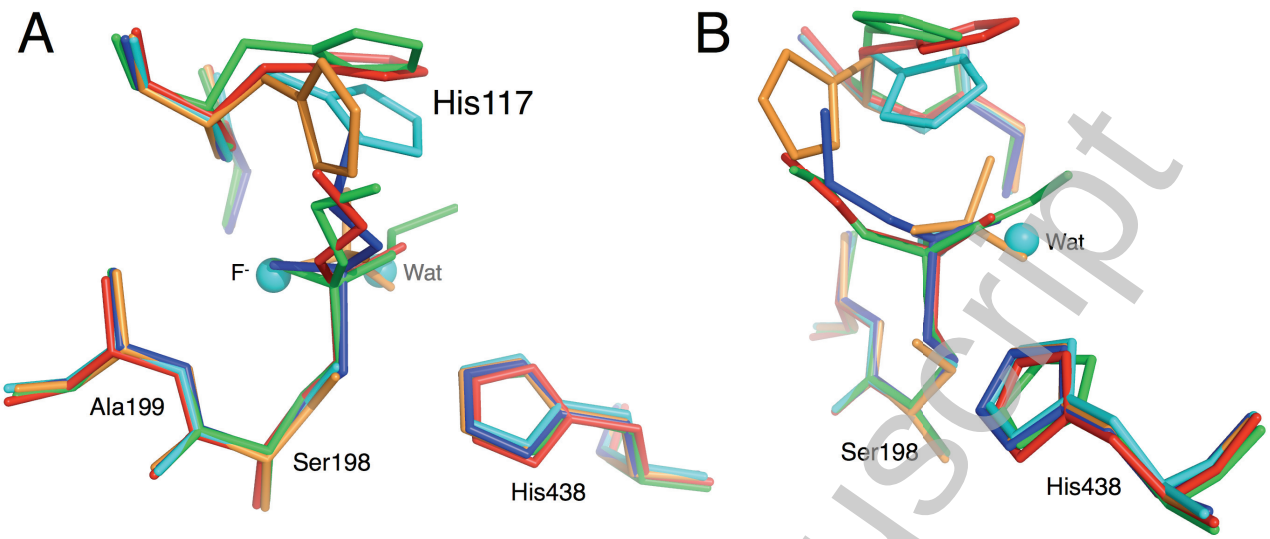

THIS IS NOT THE VERSION OF RECORD - see doi:10.1042/BJ20101648

Accepted Manuscript

Licenced copy. Copying is not permitted, except with prior permission and as allowed by law.
© 2010 The Authors Journal compilation © 2010 Portland Press Limited